Antimicrobial agent chloroxylenol targets β-catenin-mediated Wnt signaling and exerts anticancer activity in colorectal cancer

QI SUN[1*], BOXIN LIU[1*], QUANXUE LAN[2*], ZIJIE SU[1,3], QIUXIA FU[1], LIAN WANG[1], YINGYING DENG[1], CHUANLI LI[4], VIVIAN WEIWEN XUE[1], SHANSHAN LIU[1], XIANXIONG CHEN[5], GUOWU YANG[4] and DESHENG LU[1]

[1]Guangdong Provincial Key Laboratory of Regional Immunity and Diseases, International Cancer Center, Department of Pharmacology, Shenzhen University Medical School, Shenzhen, Guangdong 518060; [2]Shenzhen Longgang District Center for Disease Control and Prevention, Shenzhen, Guangdong 518100; [3]Department of Research, The Affiliated Tumor Hospital of Guangxi Medical University, Nanning, Guangxi 530021; [4]Shenzhen Academy of Metrology and Quality Inspection, National Nutrition Food Testing Center, Shenzhen, Guangdong 518102; [5]Department of Physiology, Shenzhen University Medical School, Shenzhen, Guangdong 518060, P.R. China

Received January 12, 2023; Accepted July 18, 2023

DOI: 10.3892/ijo.2023.5569

Abstract. Chloroxylenol is the active ingredient of the antibacterial agent Dettol. The anticancer effect and underlying mechanisms of this compound and other common antimicrobial agents have not been clearly elucidated. In the present study, the effects of chloroxylenol, benzalkonium chloride, benzethonium chloride, triclosan and triclocarban on β-catenin-mediated Wnt signaling in colorectal cancer were evaluated using the SuperTOPFlash reporter assay. It was demonstrated that chloroxylenol, but not the other antimicrobial agents tested, inhibited the Wnt/β-catenin signaling pathway by decreasing the nuclear translocation of β-catenin and disrupting β-catenin/T-cell factor 4 complex, which resulted in the downregulation of the Wnt target genes Axin2, Survivin and Leucine-rich G protein-coupled receptor-5. Chloroxylenol effectively inhibited the viability, proliferation, migration and invasion, and sphere formation, and induced apoptosis in HCT116 and SW480 cells. Notably, chloroxylenol attenuated the growth of colorectal cancer in the MC38 cell xenograft model and inhibited organoid formation by the patient-derived cells. Chloroxylenol also demonstrated inhibitory effects on the stemness of colorectal cancer cells. The results of the present study demonstrated that chloroxylenol could exert anti-tumor activities in colorectal cancer by targeting the Wnt/β-catenin signaling pathway, which provided an insight into its therapeutic potential as an anticancer agent.

Correspondence to: Dr Guowu Yang, Shenzhen Academy of Metrology and Quality Inspection, National Nutrition Food Testing Center, Floor 5, 4 Xili Tongfa Road, Nanshan, Shenzhen, Guangdong 518102, P.R. China
E-mail: yangguowu@smq.com.cn

Dr Desheng Lu, Guangdong Provincial Key Laboratory of Regional Immunity and Diseases, International Cancer Center, Department of Pharmacology, Shenzhen University Medical School, 1066 Xueyuan Avenue, Nanshan, Shenzhen, Guangdong 518060, P.R. China
E-mail: delu@szu.edu.cn

*Contributed equally

Abbreviations: CRC, colorectal cancer; APC, adenomatous polyposis coli; LRP6, low density lipoprotein receptor-related protein 6; DVL, Disheveled; FZD, Frizzled; CK1, casein kinase 1; TCF, T cell factor; LEF, Lymphoid-enhancing factor; CSCs, cancer stem cells

Key words: chloroxylenol, Wnt/β-catenin signaling pathway, β-catenin/T-cell factor 4, colorectal cancer

Introduction

Numerous antimicrobial agents in consumer and personal care products, including triclosan, triclocarban, benzalkonium chloride, benzethonium chloride and chloroxylenol, have become ubiquitous contaminants in the environment (1,2). Human exposure to these contaminants has gained public attention due to their biological effects such as inflammatory responses and genotoxic effects on mammals (3). However, the potential health risks and biological activities of these compounds to humans and animals remain largely unknown. Evaluation of the biological features and environmental implications of these contaminants is necessary (4,5).

Colorectal cancer (CRC) is the third most commonly diagnosed malignancy and the fourth leading cause of cancer death worldwide, with an estimated 52,550 deaths caused by colorectal cancer in 2023 (6). Although clinical diagnosis and comprehensive treatment including colonoscopy screening and targeted therapeutics in combination with chemotherapy (7,8) have greatly improved, the prognosis of patients with metastasis remains poor, with a five-year survival rate only 14% (9). Accumulating evidence suggests that cancer stem cells (CSCs) serve an important role in tumorigenesis,

drug resistance, metastasis and recurrence through internal molecular mechanisms (10-13). CSCs are a subset of cancer cells with self-renewal ability and pose a preferentially high risk of drug resistance and recurrence (10,14). Colorectal CSCs are defined by certain specific markers such as Leucine-rich G protein-coupled receptor-5 (LGR5), CD133, sex determining region Y-box 2 (SOX2) and CD44 (15,16). Therefore, drugs targeting these CSCs might effectively improve the clinical outcome of patients (17). The canonical Wnt/β-catenin signaling pathway is required for the occurrence of CRC and the maintenance of colorectal CSCs (18).

The evolutionarily conserved Wnt/β-catenin signaling pathway serves a fundamental role in determining cell differentiation, proliferation and death, and participates in the regulation of embryonic development and tissue homeostasis (19). Dysregulation of the Wnt signaling cascade has been linked to the pathogenesis of certain diseases, such as human birth defects and cancers such as CRC, melanoma and ovarian cancer (20,21). Research on genetic mutations has indicated that ~93% of patients with CRC carry somatic mutations in the genes encoding Wnt signaling components, including biallelic inactivation of adenomatous polyposis coli (APC), activating mutations in CTNNB1 and inactivating mutations in RNF43. Moreover, overexpression of the Wnt receptors Frizzled (FZD) and low-density lipoprotein receptor-related protein 5/6 (LRP5/6) is reported in CRC patients (22-24). Due to the high mutation rate of Wnt signaling pathway components and the pivotal role of Wnt signaling to support the CSC niche and plasticity in human CRCs, the development of small molecular inhibitors targeting the Wnt/β-catenin signaling pathway may have potential therapeutic effects in CRC (25).

In the Wnt/β-catenin signaling cascade, the transcriptional coactivator β-catenin is a kernel component of the pathway with its protein level and activity closely controlled by a cytoplasmic destruction complex consisting of APC, Axin, casein kinase 1 (CK1) and glycogen synthase kinase 3β (20). Binding of Wnt ligands to the FZD receptors and coreceptor LRP5/6 is deemed to be the initiation of the signal transduction pathway (26). This binding triggers the phosphorylation and recruitment of Disheveled (DVL) by activated CK1. DVL in turn inactivates the β-catenin destruction complex (27). Subsequently, depolymerization of the destruction complex renders it incapable of phosphorylating β-catenin, which leads to cytoplasmic β-catenin no longer being ubiquitinated and degraded through the ubiquitin-proteasome pathway (28). Unphosphorylated active β-catenin accumulates in the cytosol and translocates into the nucleus, interacting with transcription factors T cell-specific factor/lymphoid enhancer-binding factor (TCF/LEF) to activate transcription of downstream Wnt target genes such as c-Myc, cyclin D1, Survivin, LGR5 and Axin2 (29,30).

Chloroxylenol (para-chloro-meta-xylenol, PCMX) is a halogenated phenol widely used in antiseptic, disinfectant and cosmetic products (1). As the principal active ingredient of commonly used antiseptics, chloroxylenol exhibits its bactericidal activity primarily against Gram positive bacteria, which could be associated with its ability to decrease membrane fluidity and to interfere with the function of membrane proteins (31,32). Previous studies have reported that chloroxylenol could induce phase-transition of the cell membrane, changing it from a liquid-crystalline to a liquid-ordered phase, with increased susceptibility for bacterial membranes (31,33). Nevertheless, the anticancer effect of chloroxylenol and its underlying mechanisms are still unknown. In the present study, it was demonstrated that chloroxylenol could suppress the Wnt/β-catenin signaling pathway by inhibiting the nuclear translocation of β-catenin and blocking of the β-catenin/T-cell factor 4 interaction, thus exerting anticancer activity in CRC cells. The results demonstrated that chloroxylenol might be a novel Wnt/β-catenin signaling inhibitor with anticancer efficacy.

Materials and methods

Reagents and plasmids. Chloroxylenol was purchased from Sigma-Aldrich (Merck KGaA) and dissolved in dimethyl sulfoxide (DMSO). The SuperTOPFlash reporter vector was donated by Dr Karl Willert (University of California at San Diego, USA). Activator protein 1-Luc (AP1-Luc) and nuclear factor of activated T cells-Luc (NFAT-Luc) reporters were purchased from BD Biosciences. The expression plasmids encoding β-catenin, β-catenin 4A, TCF4E and β-galactosidase (β-gal) and pDKK4-Luc reporter have been described previously (34).

Cell culture. The human embryonic kidney 293T cells, colorectal cancer HCT116 and SW480 cell lines, and mouse colon cancer MC38 cells were purchased from the American Type Culture Collection. Cells were maintained in Dulbecco's Modified Eagle's Medium (DMEM; Thermo Fisher Scientific, Inc.) supplemented with 1% penicillin-streptomycin and 10% fetal bovine serum (FBS; Gibco; Thermo Fisher Scientific, Inc.) in a humidified incubator at 37˚C with 5% CO_2. The cultured cells were tested for mycoplasma every month to ensure that they are not contaminated using a luciferase mycoplasma detection kit (cat. no. FM301-02-V2, Transgen, Inc.). The authenticity of the cell lines was confirmed using STR profiling.

Transfection and luciferase reporter gene assays. For the luciferase reporter assays, 293T cells were transferred to 24-well plates pre-coated with 1% poly-D-lysine at 37˚C for 24 h, prior to use for the SuperTopFlash or DKK4-Luc assays. Colorectal cancer cells (HCT116 and SW480) were transfected with 0.25 μg SuperTOPFlash or SuperFOPFlash (negative control) reporters along with control plasmid pCMXβgal (0.05 μg) in three replicates. 293T cells were transiently transfected with SuperTOPFlash reporter (0.25 μg) or pDKK4-Luc (0.25 μg) reporter along with transfection control plasmid pCMXβgal (0.05 μg), and β-catenin, β-catenin 4A, β-catenin 4A/TCF4E or pcDNA3.1 (0.15 μg) expression plasmids. The promoter region of SuperTOPflash reporter gene contained 8 duplicate TCF/LEF transcription factor binding sites and the expression level of luciferase represented the activation level of the Wnt signaling pathway. SuperFOPFlash is a negative control reporter gene of SuperTOPFlash. It was constructed by inserting 8 duplicate mutant TCF/LEF binding site sequences into its polyclonal sites. Cell lysates were used for SuperTOPFlash or SuperFOPFlash luciferase activity assessment after 24 h drug treatment using a Luciferase assay

kit (cat. no. E1501; Promega Corporation). The luciferase values were normalized to β-galactosidase (β-gal) activity following detection using a Gal-Screen kit (cat. no. T1028; Thermo Fisher Scientific, Inc.) according to the manufacture's protocol. For immunoprecipitation experiments with 293T cells, transfections were performed in 10 cm dishes using 1 μg of pcDNA or expression plasmids encoding β-catenin and TCF4E. Following chloroxylenol treatment, protein collection was performed. All transfections were performed using Lipofectamine® 3000 (Invitrogen; Thermo Fisher Scientific, Inc.) according to the manufacturer's protocols at 37˚C for 24 h. Twenty four hours after transfection, cells were treated with a range of concentrations of antimicrobial agents and assessed with subsequent assays.

Immunoblotting. Colorectal cancer HCT116 and SW480 cells were initially collected with a scraper and then centrifuged at 150 x g at 4˚C for 5 min and lysed in lysis buffer consisting of 20 mM Tris-HCl (pH 7.4), 150 mM NaCl, 2.5 mM sodium pyrophosphate, 1 mM EDTA, 1 mM EGTA, 1 mM PMSF, 1% Triton X-100, 1 mM β-glycerol phosphate, 1 mM sodium orthovanadate and 2 μg/ml leupeptin, followed by sonication on ice, with a power of 15% and a lysis time of 1 min (sonication for 2 sec, rest for 4 sec). A BCA protein assay kit (Cell Signaling Technology, Inc.) was then used to assess the concentration of the protein. Equal amounts of 20-40 μg per lane proteins were then separated using SDS-PAGE on an 8% SDS-polyacrylamide gel and transferred to PVDF (MilliporeSigma). Western blotting was performed at 4˚C overnight with primary antibodies as follows: Anti-V5 (1:1,000; cat. no. 13202S; Cell Signaling Technology, Inc.), anti-Flag (1:1,000; cat. no. 14793S; Cell Signaling Technology, Inc.), anti-non-phospho active β-catenin (1:2,000; cat. no. 8814; Cell Signaling Technology, Inc.), anti-TCF4 (1:2,000; cat. no. 2569; Cell Signaling Technology, Inc.), anti-LGR5 (1:1,000; cat. no. ab273092; Abcam), anti-SOX2 (1:1,000; cat. no. 23064S; Cell Signaling Technology, Inc.), anti-β-catenin (1:2,000; cat. no. Sc-7963; Santa Cruz Biotechnology, Inc.), anti-mLGR5 (1:1,000; cat. no. DF2816; Affinity Biosciences, Ltd.), anti-GAPDH (1:5,000; cat. no. 60004-1-Ig; Proteintech Group, Inc.) and anti-β-actin (1:5,000; cat. no. HC201-01; TransGen Biotech Co., Ltd.). Blocking was performed before incubation with primary antibody using 5% non-fat powdered milk (Sangon Biotech Co., Ltd.) at room temperature for 1 h. The washing solution was prepared by adding 0.1% Tween 20 to TBS solution. The PVDF membranes were then incubated for 1 h at room temperature with relevant HRP-conjugated goat anti-mouse (1:10,000; cat. no. A16066; Thermo Fisher Scientific, Inc.) or HRP-conjugated goat anti-rabbit (1:10,000; cat. no. A16096; Thermo Fisher Scientific, Inc.) IgG secondary antibodies. The blots were visualized using Tanon 5200 Chemiluminescent Imaging System (Tanon Science and Technology Co., Ltd.,) or X-ray film (Kodak) after incubation with ECL Plus Western Blotting Substrate (Thermo Fisher Scientific, Inc.). The intensity of the was semi-quantified using ImageJ 1.8.0 (National Institutes of Health).

Immunoprecipitation. Total protein was extracted from 293T or HCT116 cells using 500 μl of RIPA buffer which contained a cocktail of protease inhibitors and phosphatase inhibitors. After quantification of the lysate protein concentration using a BCA protein assay kit (Cell Signaling Technology, Inc.), proteins were incubated with 2 μg anti-β-catenin (1:250; cat. no. Sc-7963; Santa Cruz Biotechnology, Inc.) or anti-Flag (1:250; cat. no. 14793S; Cell Signaling Technology, Inc.) antibodies and protein A/G agarose beads overnight at 4˚C. Beads were washed four times with 700 μl RIPA buffer, heat denatured at 95˚C for 5 min followed by gel electrophoresis on a 9% SDS-PAGE gel. For subcellular separation, a Subcellular Protein Fractionation Kit (Thermo Fisher Scientific, Inc.) was used to separate the cytoplasmic and nuclear parts according to the manufacturer's instructions. GAPDH and Histone H3 were used as the cytoplasmic and nuclear markers, respectively. The expression of GAPDH and Histone H3 was detected by immunoblotting with anti-GAPDH (1:5,000; cat. no. 60004-1-Ig; Proteintech Group, Inc.) and anti-Histone H3 antibodies (1:5,000; cat. no. 9715; Cell Signaling Technology, Inc.). The PVDF membranes were incubated for 1 h at room temperature with the aforementioned HRP-conjugated secondary antibodies.

Immunofluorescence staining. Cells were plated in 12-well plates at a density of 70-80% and allowed to grow for 24 h in the cell incubator at 37˚C. After treatment with chloroxylenol at 37˚C for 24 h, the cells were fixed with 4% paraformaldehyde at room temperature for 15 min and permeabilized with 0.4% TritonX-100. After blocking with blocking buffer (5% non-fat powdered milk and 0.1% Tween20 dissolved in TBS) at room temperature for 2 h, the cells were incubated with anti-β-catenin antibodies (1:200; cat. no. Sc-7963 Santa Cruz Biotechnology, inc.) for 2 h at room temperature. Alexa Fluor488-conjugated goat anti-mouse IgG antibodies (1:200; cat. no. Z-25402; Molecular Probes; Thermo Fisher Scientific, Inc.) were used as a secondary antibody and incubated at 37˚C for 1 h and DAPI was used to visualize the nucleus with an incubation time of 5 min at room temperature. The slides were imaged using a Leica TCSSP5II laser scanning confocal microscope (Leica Microsystems GmbH). Acquisition settings were as follows: DAPI, excitation/emission at 358/461 nm and β-catenin, excitation/emission at 495/519 nm. Images were analyzed using Leica LASA Flite software (Leica Application Suite X; version 2.6.0; Leica Microsystems GmbH).

Reverse transcription-quantitative PCR (RT-qPCR) analyses. RNAiso Plus (Takara Bio, Inc.) was used to isolate total RNA, which then reverse transcribed into cDNA according to the manufacturer's protocol (37˚C for 15 min, 85˚C for 5 sec) using the Primescript RT reagent kit (Takara Bio, Inc.). Quantitative PCR analyses (95˚C for 5 min; 95˚C for 15 sec, 60˚C for 1 min) on the prepared cDNA were then performed using FastStart Universal SYBR-Green Master (Selleck Chemicals). The comparative $2^{-\Delta\Delta Cq}$ method was used to evaluate the relative expression of the genes (35). The primer sequences used were as follows: Axin2 sense (S), 5'-TACACTCCTTATTGGGCGATCA-3' and antisense (AS), 5'-TTGGCTACTCGTAAAGTTTTGGT-3'; Survivin S, 5'-AGGACCACCGCATCTCTACAT-3' and AS, 5'-AAGTCTGGCTCGTTCTCAGTG-3'; LGR5 S, 5'-CTCCCAGGTCTGGTGTGTTG-3' and AS, 5'-GAGGTCTAGGTAGGAGGTGAAG-3'; GAPDH S; 5'-CCAGAACATCATCCCTGCCTCTACT-3' and AS, 5'-GGTTTTTCTAGA

CGGCAGGTCAGGT-3'; mouse (m)Axin2 S, 5'-ATGAGT AGCGCCGTGTTAGTG-3' and AS, 5'-GGGCATAGGTTT GGTGGACT-3', mSOX2 S, 5'-GCGGAGTGGAAACTTTTG TCC-3' and AS, 5'-GGGAAGCGTGTACTTATCCTTCT-3'; mLGR5 S, 5'-ACATTCCCAAGGGAGCGTTC-3' and AS, 5'-ATGTGGTTGGCATCTAGGCG-3', mSurvivin S, 5'-GAG GCTGGCTTCATCCACTG-3'; AS, 5'-ATGCTCCTCTAT CGGGTTGTC-3'; and mGAPDH S, 5'-AGGTCGGTGTGA ACGGATTTG-3 and AS, 5'-GGGGTCGTTGATGGCAAC A-3'.

Chromatin immunoprecipitation (ChIP) assays. A ChIP-IT Express Enzymatic Chromatin Immunoprecipitation Kit (Active Motif, Inc.) was used for ChIP assays according to the manufacturer's protocols. Briefly, HCT116 and SW480 cells were treated with chloroxylenol for 24 h at 37˚C. After crosslinking with 1% formaldehyde for 10 min at room temperature and termination with 125 mM glycine, the cells were washed, lysed with RIPA buffer at 4˚C for 10 min and sonicated to reduce the DNA fragment length to 300-600 bp. The chromatin complexes were incubated with 2 μg mouse antibodies against β-catenin (1:50; cat. no. Sc-7963; Santa Cruz Biotechnology, Inc.) or mouse IgG (1:50; cat. no. Sc-2025; Santa Cruz Biotechnology, Inc.) and protein A/G agarose at 4˚C overnight. The complexes were then precipitated by centrifugation at 4˚C, 7,000 x g for 1 min, eluted and treated with Protease K. The DNA in the precipitated complex was extracted with Chelex100 (Bio-Rad Laboratories, Inc.) and then detected using qPCR. qPCR analyses (95˚C for 5 min; 95˚C for 15 sec, 60˚C for 1 min) on the prepared DNA were then performed using FastStart Universal SYBR-Green Master (Selleck Chemicals). The comparative $2^{-\Delta\Delta Cq}$ method was used to evaluate the relative expression of the genes (35). The following primers for the putative β-catenin binding site in Survivin, Axin2, Sox2 and LGR5 promoter regions, which had been confirmed in our previous study (36), were used for amplification. The primer sequences used were as follows: Survivin S, 5'-GCGTTCTTTGAAAGCAGT-3' and AS, 5'-ATCTGGCGGTTAATGGCG-3'; Axin2 S, 5'-CGGTTG GCGAAAGTTTGC-3' and AS, 5'-GGACTCGGGAGCCTA AAGGT-3'; LGR5 S, 5'-ACCACCTCTTTCAGCAGCTC-3' and AS, 5'-GAACTGAGAGCAGTCCCACC-3'; and SOX2 S, 5'-AATACGAGTTGGACAGCCGC-3' and AS, 5'-TTTGTA TCCCCTCTCGCAGC-3'.

Cell viability and proliferation assays. Cells were plated in 96-well plates at a density of $2x10^4$ cells per well and then treated with the indicated concentrations of chloroxylenol for 24 h. For the viability assay, the cells were cultured for another 4 h with fresh medium containing 0.5 mg/ml MTT at 37˚C. After the medium was removed, formazan crystals were dissolved in DMSO and the absorbance of formazan solution was quantified at 490 nm with 570 nm used as a reference. For cell proliferation evaluation, the bromodeoxyuridine (BrdU) incorporation assay was performed using the Cell Proliferation ELISA BrdU Chemiluminescent Kit (Roche Diagnostics) according to the manufacturer's protocols.

Colony formation assays. Cells were added to six-well plates at a cell density of $1x10^3$ cells per well, and then incubated in medium containing 10% FBS with the indicated concentrations of chloroxylenol at 37˚C in a humidified incubator with 5% CO_2. After 10 days of incubation, cells were fixed with 4% paraformaldehyde at room temperature for 15 min, stained with 0.1% crystal violet at room temperature for 20 min and imaged using a DP74 light microscope (Olympus Corporation). Colonies were counted and quantified manually to support subsequent statistical analysis.

Transwell assays. Transwell assays were utilized to perform *in vitro* cell migration and invasion assessments as previously described (37). Briefly, $2x10^5$ cells were suspended in 100 μl serum-free medium containing the indicated concentrations of chloroxylenol and then seeded into 24-well Transwell chambers with 8-μm pore size membranes. The lower chamber medium containing 20% FBS acted as a chemoattractant, while the upper chamber contained DMEM medium without FBS. After incubation at 37˚C for 12 h, the cells on the upper side membrane that had not migrated were removed. The migrated cells were stained with 0.1% crystal violet for 15 min at room temperature and then imaged using a DP74 light microscope (Olympus Corporation). With regard to invasion assay, the procedure was the same as for the cell migration assay except that the Transwell chambers with 8 μm pore size membranes were precoated with Matrigel (Corning Life Sciences) at 4˚C and incubated at 37˚C for 3 h. Stained cells were rinsed with 33% acetic acid at room temperature for 10 min and then the absorbance of the resulting solution was assessed at 570 nm for quantitative analysis.

Flow cytometric analyses. After treatment with chloroxylenol (62.5-250 μM) at 37˚C for 24 h or 48 h, HCT116 and SW480 cells were collected. Quantitative fluorescence sorting was performed using a FACSCalibur™ (BD Biosciences) fluorescence-activated cell sorting instrument and FlowJo v10.0.8 (Tree Star, Inc.) for subsequent analyses. For the apoptosis assay, cells were treated with Annexin V-fluorescein isothiocyanate and propidium iodide solution (TransGen Biotech Co., Ltd.) according to the manufacturer's protocols. To test the stemness of CRC cells, SW480 cells were stained with PE-conjugated anti-human LGR5 antibodies (1:100; cat. no. 563470, BD Biosciences) at room temperature for 45 min.

Sphere formation assays. HCT116 cells were seeded at 250 cells per well into the sphere culture medium MammCult (Stemcell Technologies, Inc.) with the indicated concentrations of chloroxylenol in a 24-well plate. After 10 days of incubation at 37˚C, spheres with a diameter >50 μm were tallied manually and microphotographed using a DP74 light microscope (Olympus Corporation).

Human tissue samples and organoid culture. The present study was approved by The Research Ethics Committee of Shenzhen University (approval no. PN-2022-001) and the patient agreed and signed written informed consent. The tissues of a CRC patient in the First Affiliated Tumor Hospital of Guangxi Medical University confirmed by colonoscopy biopsy were included in the present study. The patient had not received any anti-cancer therapy before CRC biopsies were taken. Human CRC biopsies were washed with PBS

and incubated on ice in a mixture of antibiotics for 30 min and 2 mM EDTA/PBS for 60 min to remove normal epithelial cells. Tissues were cut into small pieces and digested enzymatically in digestion buffer (2.5% FBS, 200 U/ml type IV collagenase, 125 μg/ml type II dispersase) at 37˚C for 1 h with continuous shaking in a water bath. The tumor samples were then embedded in Matrigel on ice and seeded in a preheated 24-well plate. After polymerization at 37˚C for 15 min, 500 μl advanced DMEM/F12 containing 50 ng/ml EGF, 50 ng/ml noggin, 500 ng/ml R-spondin 1, 100 ng/ml Wnt3a, 10 mM nicotinamide, 1 mM N-acetylcysteine, and 10 μM Y-27631 was added and replaced every two to three days.

Animal model study. All animal experimental protocols were approved by the Animal Ethics Committee of Shenzhen University (approval no. AEWC-2021006). Male C57BL/6 mice were purchased from the Guangdong Medical Laboratory Animal Center. The animals were acclimatized to the laboratory for at least 1 week prior to the start of the experiments. All mice were housed in a specific-pathogen-free facility at the Animal Research Center of Shenzhen University, with five mice per cage under a 12:12 h light/dark cycle at a constant temperature of 24˚C with 50-60% relative humidity and fed a standard rodent diet with free access to sterile water, which was replaced every day. Ten mice were included in the present study and the mice were anesthetized with isoflurane inhalation at a concentration of 3-5% in oxygen and maintained at 1-2% during the surgery. At the end of the experiments, euthanasia was performed by CO_2 asphyxiation with CO_2 displacement rate at 60% of the container volume per min. Death was confirmed by checking for the cessation of heartbeat and respiration. Any animal which showed maximum tumor volume >750 mm^3 or rapid loss of 15-20% of original body weight or signs of cachexia and persistent muscle wasting even without weight loss, was euthanized. In animal studies, both the carer of the animals and the assessor of the results were blinded.

For the colorectal cancer xenograft mouse model, mouse colon cancer MC38 cells were subcutaneously implanted into the right flank of 7-week-old male C57BL/6 mice at $2x10^6$ cells/100 μl of PBS per mouse. Tumor growth was monitored daily and measured on alternate days after implantation. When the tumor size reached ~50 mm^3, ten mice were randomly divided into two groups (5 mice/group) and treated with vehicle (8% ethanol/12% polyethylene glycol in saline) or 5 mg/kg chloroxylenol in the vehicle via intraperitoneal injection every other day. Tumor volume was measured using calipers on alternate days and calculated using the formula: 0.528 x (length/2) x $(width/2)^2$. After two weeks of treatment, the mice were sacrificed, and the tumors were excised and weighed. For RNA and protein analyses, tumor tissues were homogenized, and RNA or protein was extracted. RT-qPCR and western blot assays were performed according to the aforementioned methods. For histological analysis, tumors were fixed in formalin at room temperature for 24 h, embedded in paraffin and sectioned to 5 μm slices. Hematoxylin and eosin (H&E) staining and immunohistochemical analysis were performed as previously described (37).

Data and statistical analyses. Data were presented as mean ± SD. GraphPad Prism software (v8.0; GraphPad software; Dotmatics) was used for statistical analysis. On the basis of their distribution, data were analyzed by one-way analysis of variance followed by Dunnett's t-test or Student's t-test. $P<0.05$ was considered to indicate a statistically significant difference.

Results

Inhibition of Wnt/β-catenin signaling by chloroxylenol. To identify novel small molecules that modulated the Wnt/β-catenin signaling pathway, a cell-based SuperTOPFlash reporter system was used to screen a known-compound library. Preliminary screening results demonstrated that chloroxylenol could inhibit β-catenin-mediated Wnt signaling in 293T cells. As chloroxylenol is a frequently used antimicrobial compound, the effects of several common antimicrobial agents, in health care products, on the Wnt/β-catenin signaling pathway in 293T cells were assessed in the present study. Only chloroxylenol demonstrated a dose-dependent inhibitory effect on the activity of the SuperTOPFlash reporter activated by Wnt1 and LPR6 (Fig. S1A and B), while benzethonium chloride (Fig. S1C and D), benzalkonium chloride (Fig. S1E and F), triclosan (Fig. S1G and H) and triclocarban (Fig. S1I and J) demonstrated not significant effect on the SuperTOPFlash reporter in 293T cells, even at toxic doses. In control experiments, Wnt inhibiting concentrations of chloroxylenol had no effect on the luciferase activity of an activator protein 1 (AP-1) reporter gene (Fig. S2A) or a nuclear factor of activated T cells (NFAT) reporter gene (Fig. S2B).

As aberrant activation of the Wnt/β-catenin signaling pathway is common in CRC (38), the effect of chloroxylenol on Wnt/β-catenin signaling in CRC cells was further assessed. SW480 and HCT116 cells were transfected with the SuperTOPFlash reporter. Treatment with 31.25-250 μM chloroxylenol in HCT116 and SW480 cells significantly inhibited the transcriptional activity of SuperTOPFlash reporter, but had little effect on the activity of SuperFOPFlash reporter (Fig. 1A and B). In HCT116 cells, the activity of SuperTOPFlash reporter showed a downward trend with the treatment of 31.25-125 μM chloroxylenol. In SW480 cells, although the downward trend was not significant, treatment with chloroxylenol significantly reduced the SuperTOPFlash activity compared with the untreated group. At doses of toxic concentration, benzalkonium chloride (2.5-5 μM; Fig. 1E and F) and triclosan (10 μM; Fig. 1G and H) also demonstrated a significant decrease in SuperTOPFlash activity. However, at non-toxic concentrations, benzethonium chloride (0-1.25 μM; Fig. 1C and D), benzalkonium chloride (0-1.25 μM; Fig. 1E and F), triclosan (0-5 μM; Fig. 1G and H) and triclocarban (0-5 μM; Fig. 1I and J) did not significantly affect the transcription of the SuperTOPFlash reporter in CRC cells. Moreover, the mRNA expression levels of certain Wnt target genes in HCT116 and SW480 cells were quantified using RT-qPCR assays to further determine the effect of chloroxylenol on β-catenin-mediated transcription in CRC cells. In HCT116 cells, concentrations of 125-250 μM chloroxylenol could exert a significant decrease in mRNA levels of Axin2 and LGR5, while for Survivin, there was only a significant decrease at 250 μM. In SW480 cells, Axin2 demonstrated

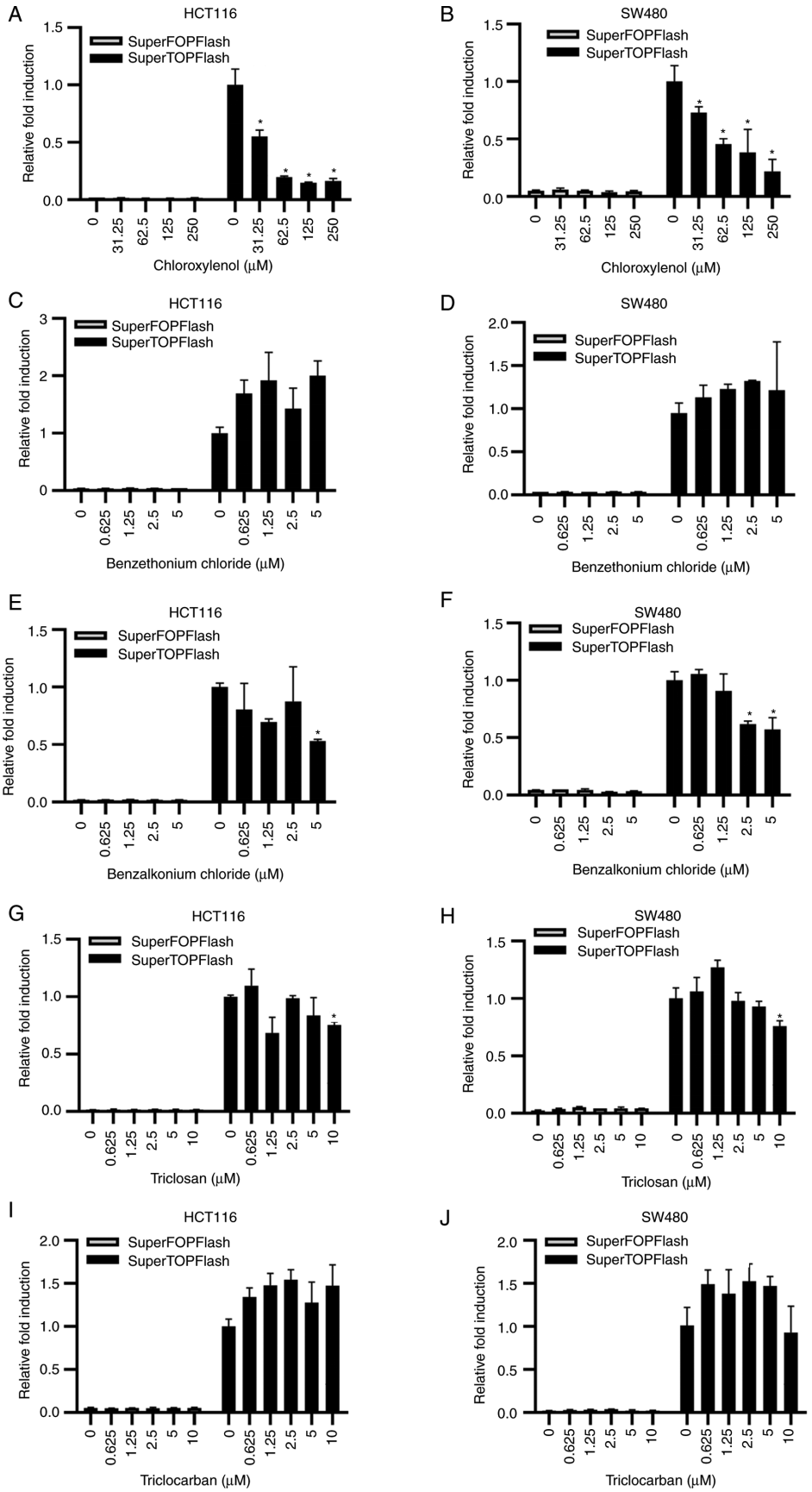

Figure 1. Chloroxylenol, but not its analogs, inhibits the Wnt/β-catenin signaling pathway. (A) HCT116 and (B) SW480 CRC cells were transfected with SuperTOPFlash vector or negative control SuperFOPFlash for 24 h prior to treatment with chloroxylenol at the indicated concentrations. The luciferase activities were normalized to β-gal signal. (C) HCT116 and (D) SW480 CRC cells were treated with benzethonium chloride at the indicated concentrations for 24 h and the luciferase activity was assessed. (E) HCT116 and (F) SW480 CRC cells were treated with benzalkonium chloride at the indicated concentrations for 24 h and the luciferase activity was assessed. (G) HCT116 and (H) SW480 CRC cells were treated with triclosan at the indicated concentrations for 24 h and the luciferase activity was assessed. (I) HCT116 and (J) SW480 CRC cells were treated with triclocarban at the indicated concentrations for 24 h and the luciferase activity was assessed. Data are presented as mean ± SD. n=3. *P<0.05 vs. control (0 μM) group. CRC, colorectal cancer.

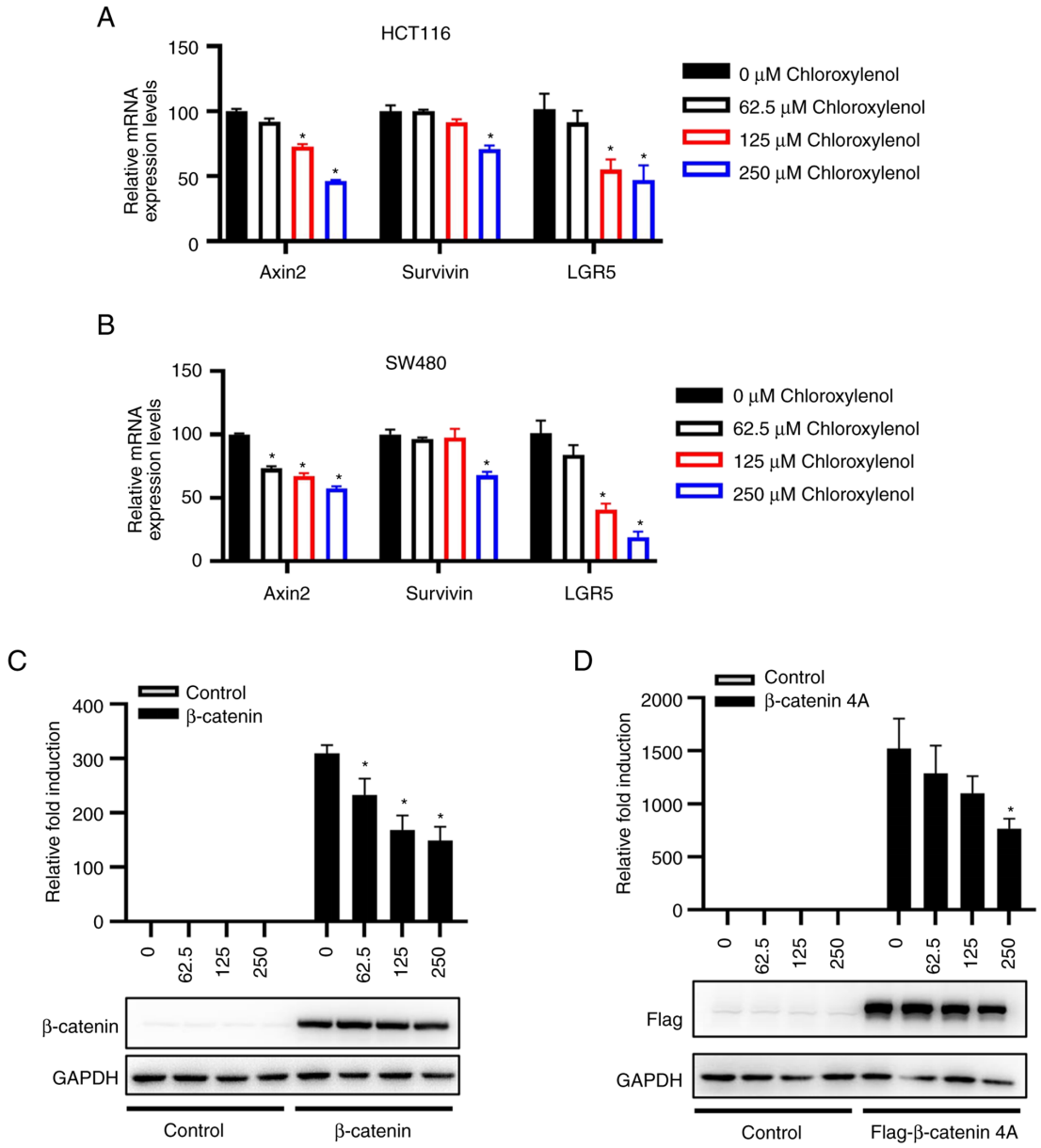

Figure 2. Chloroxylenol inhibits the β-catenin-mediated Wnt signaling. (A) HCT116 and (B) SW480 cells were treated with chloroxylenol for 24 h. Total RNA was extracted and then reverse-transcribed into cDNA. qPCR of the cDNA was performed to assess the mRNA expression levels of Axin2, Survivin and LGR5 compared with DMSO treated control cells. The SuperTOPFlash reporter gene was transfected into 293T cells together with empty vector or expression plasmids encoding (C) β-catenin or (D) β-catenin 4A. The luciferase values were normalized to β-gal activities. The protein expression level of β-catenin or β-catenin 4A corresponding to the transfection experiment is presented below the bar chart. Data are presented as mean ± SD. n=3. *P<0.05 vs. control (0 μM) group. cDNA, complementary DNA

a significant decrease within the concentration range of 62.5-250 μM, while LGR5 and Survivin decreased at 125 and 250 μM treatment, respectively (Fig. 2A and B). These results demonstrated the antagonistic effect of chloroxylenol on the Wnt/β-catenin signaling cascade in CRC cells.

HCT116 cells carry an S45 mutation in β-catenin and SW480 cells harbor an APC deletion at the C terminus at residue 1338, this suggested that chloroxylenol might exert its antagonistic effect via targeting downstream of APC and β-catenin in the Wnt signaling pathway in CRC cells. To evaluate this hypothesis, β-catenin and its N-terminal mutant β-catenin 4A along with SuperTOPFlash reporter were transfected into 293T cells. The expression plasmid of β-catenin 4A was previously constructed by mutating four serine and threonine residues (Ser-33, Ser-37, Thr-41 and Ser-45) in the N-terminal of β-catenin to alanine, which indicated the persistent activation of the Wnt signaling cascade (36,39). The results demonstrated that chloroxylenol significantly inhibited the transcriptional activity mediated by both wild type β-catenin and β-catenin 4A, which suggested that chloroxylenol may act downstream of the Wnt signaling pathway (Fig. 2C and D).

Chloroxylenol prevents nuclear translocation of β-catenin in CRC cells. β-catenin, a key component of the Wnt signaling pathway, is tightly regulated at three hierarchical levels; protein stability, subcellular localization and transcriptional activity (40). To elucidate the mechanism underlying the inhibitory effect of chloroxylenol on Wnt signaling, its effect

on the protein expression level of β-catenin was assessed. Quantitative analysis of the β-catenin protein expression level demonstrated that chloroxylenol had no significant effect on the protein expression level of β-catenin in HCT116 and SW480 cells (Fig. 3A and B). Furthermore, an immunofluorescence staining assay was performed to determine the effect of chloroxylenol on the subcellular localization of β-catenin. Chloroxylenol markedly decreased nuclear localization of β-catenin in HCT116 and SW480 cells (Fig. 3C and D). Subcellular localization analysis further demonstrated that chloroxylenol treatment could significantly decrease the accumulation of β-catenin in the nucleus, accompanied by a marked increase in the levels of cytoplasmic β-catenin in SW480 cells and a significant increase in the levels of cytoplasmic β-catenin in HCT116 cells (Fig. 3E and F).

Chloroxylenol inhibits β-catenin/TCF4 mediated transcriptional activity and interferes with the interaction of β-catenin with TCF4E. The transcription factor TCF/LEF recruits β-catenin to the promoter region of Wnt target genes to activate gene transcription. ChIP assays were performed to determine the effect of chloroxylenol on the binding of β-catenin to the promoter region of Wnt downstream target genes Axin2 and Survivin. The results demonstrated that chloroxylenol treatment significantly reduced β-catenin binding to Axin2 and Survivin promoter region in both HCT116 (Fig. 4A and B) and SW480 cells (Fig. 4C and D).

To assess the effect of chloroxylenol on β-catenin-mediated transcriptional activity, the pDKK4-Luc reporter was constructed by cloning the DKK4 promoter with five putative TCF-binding sites into a luciferase reporter vector as previously described (41). The simultaneous presence of β-catenin and TCF4 is required for the activation of the pDKK4-Luc reporter (42). 293T cells were transfected with pDKK4-Luc reporter and expression vectors encoding β-catenin 4A, TCF4E and β-catenin 4A/TCF4E, respectively. The results illustrated that the expression of β-catenin 4A/TCF4E activated the transcriptional activity of the pDKK4-Luc reporter, and chloroxylenol treatment reduced β-catenin 4A/TCF4E-mediated reporter activity in a dose dependent manner (Fig. 4E).

Next, the effect of chloroxylenol on the interaction between β-catenin and TCF4E was evaluated. The expression plasmids encoding Flag-β-catenin 4A and TCF4E-V5 were transfected into 293T cells, and Flag-β-catenin 4A was co-immunoprecipitated with an anti-Flag agarose, followed by immunoblotting analyses. The results demonstrated that Flag-β-catenin 4A was specifically coprecipitated with TCF4E-V5, and the interaction was significantly reduced upon chloroxylenol treatment (Fig. 4F). The effect of chloroxylenol on the interaction between β-catenin and TCF4E was further assessed in HCT116 cells. The results demonstrated that endogenous β-catenin and TCF4E were specifically co-immunoprecipitated by anti-β-catenin antibodies and chloroxylenol treatment decreased the β-catenin/TCF4E interaction in a dose-dependent manner (Fig. 4G).

Chloroxylenol represses the viability, proliferation, migration and invasion of CRC cells, and induces apoptosis in CRC cells. To assess the cytotoxicity of chloroxylenol against CRC cells, an MTT assay was performed. HCT116 and SW480 cells were treated with 62.5-1,000 μM chloroxylenol for 48 h. After 4 h of incubation with MTT, formazan solution was measured at 490 nm to evaluate the relative cell viability. The experimental results indicated that chloroxylenol effectively reduced the viability of CRC cells, with IC_{50} values of 280.8 μM in HCT116 and 378.5 μM in SW480 cells (Fig. 5A and B). A BrdU cell proliferation assay was used to assess the proliferation of CRC cells. Chloroxylenol treatment significantly repressed the proliferation of HCT116 and SW480 cells (Fig. 5C and D). Furthermore, colony formation assays were performed which demonstrated that chloroxylenol significantly decreased the number of colonies formed by HCT116 and SW480 cells (Fig. 5E), which illustrated that chloroxylenol could effectively block the colony formation of CRC cells. The effect of chloroxylenol on apoptosis in HCT116 and SW480 cells was also assessed. Apoptotic cells were detected using flow cytometry after treatment with different concentrations of chloroxylenol ranging from 62.5-250 μM for 24 h or 48 h. The results demonstrated that 250 μM chloroxylenol significantly induced apoptosis in CRC cells (Figs. 5F and S3).

Considering the importance of Wnt/β-catenin signaling in the migration and invasion of cancer cells, Transwell assays were used to assess the *in vitro* migration and invasion ability of CRC cells in response to a range of concentrations of chloroxylenol. In the presence of 20% FBS as a chemoattractant, migration was evaluated by counting those cells that had migrated. For invasion assays, Matrigel-coated chambers were used. Chloroxylenol at 125 μM exerted a significant inhibitory effect on the migration and invasion of HCT116 cells (Fig. 5G). In SW480 cells, chloroxylenol also significantly suppressed invasion, but the inhibition of migration was not significant (Fig. 5H).

Suppression of stemness by chloroxylenol in CRC cells. The Wnt/β-catenin signaling cascade serves a fatal role in the maintenance of cancer cell stemness. A sphere formation assay was performed to analyze the effect of chloroxylenol on the stemness of HCT116 cells. The number and size of the spheres was remarkably reduced after 10 days of incubation with 125 μM chloroxylenol (Fig. 6A). SOX2 and LGR5 are well-known CRC stem cell markers (15,43). The protein expression levels of SOX2 and LGR5 were significantly decreased after chloroxylenol treatment in HCT116 and SW480 cells (Fig. 6B and C). Furthermore, ChIP assays were performed to test whether chloroxylenol has any effect on the binding of β-catenin to the promoter regions of LGR5 and SOX2. The results demonstrated that chloroxylenol treatment decreased β-catenin binding to the promoters of LGR5 or SOX2 in HCT116 cells (Fig. 6D and E), which suggested that chloroxylenol-mediated β-catenin nuclear translocation may lead to reduced expression of LGR5 and SOX2. Human colon cancer cells with LGR5-positive have been reported to serve as CSCs in growing cancer tissues (16). Flow cytometric analysis demonstrated that the number of LGR5-positive cells was significantly decreased when SW480 cells were treated with chloroxylenol (Fig. 6F). Taken together, these results demonstrated that chloroxylenol effectively blocked sphere formation of CRC cells and decreased protein expression levels of the stemness markers LGR5 and SOX2, which indicated the suppressive effect of chloroxylenol on CRC stemness.

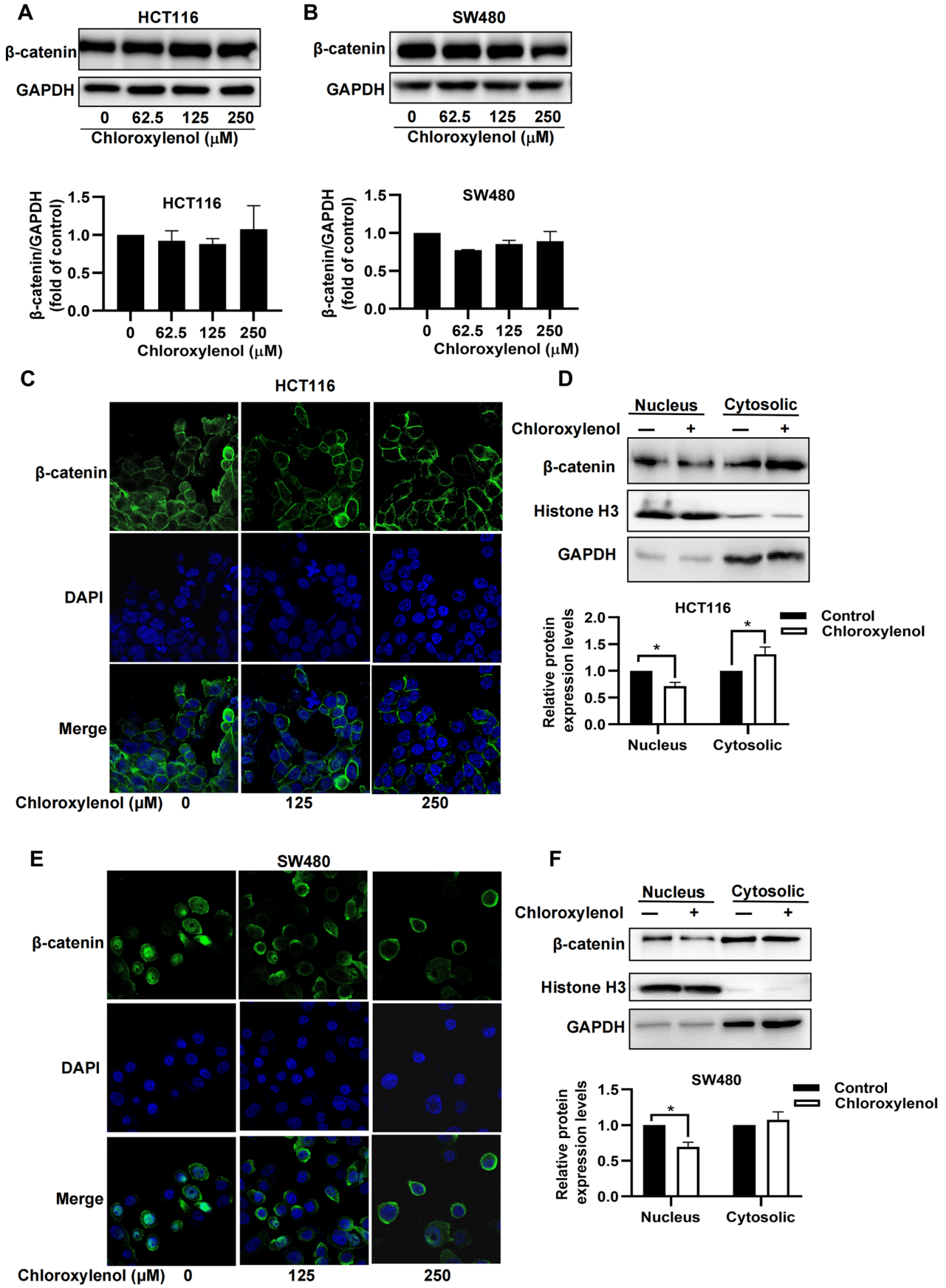

Figure 3. Chloroxylenol prevents β-catenin nuclear translocation in CRC cells. (A) HCT116 and (B) SW480 cells were treated with DMSO or chloroxylenol for 24 h. The protein expression level of β-catenin was assessed using western blotting. Densitometric quantification of the protein bands was presented in the lower panel (n=3). (C) HCT116 and (E) SW480 cells were treated with the indicated concentrations of chloroxylenol for 24 h the cells were then fixed and subjected to immunofluorescence staining. After 24 h of chloroxylenol treatment, subcellular components of (D) HCT116 and (F) SW480 cells were separated, and then assessed using western blotting. The lower panels of D and F presented the quantitative analysis of western blot bands. Data are presented as mean ± SD. n=3. *P<0.05 vs. control (0 μM) group.

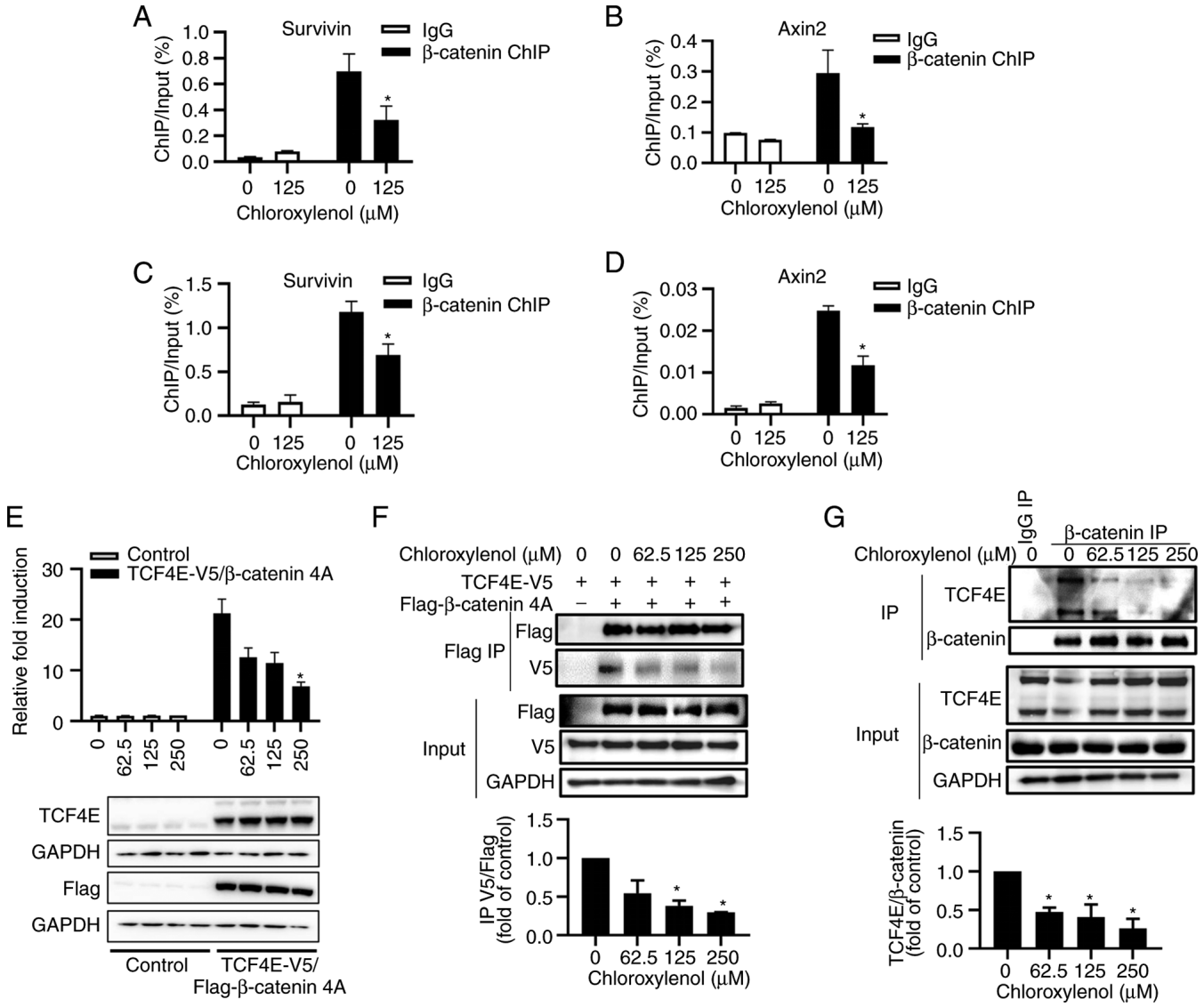

Figure 4. Chloroxylenol inhibits β-catenin/TCF4 mediated transcriptional activity and interferes with the interaction of β-catenin and TCF4E. (A and B) HCT116 and (C and D) SW480 cells were treated with chloroxylenol or DMSO for 24 h, followed by cross-linking fixation, immunoprecipitation, affinity purification and quantitative PCR assays. (E) The 293T cells were transfected with pDKK4-Luc reporter as well as empty vector or expression plasmids for β-catenin 4A/TCF4E. Cells were then incubated with DMSO or chloroxylenol for 24 h. Luciferase values were normalized to β-gal activity. The protein expression level of TCF4E or β-catenin 4A, according to the transfection experiment was confirmed by western blotting, below the bar chart. (F) Expression plasmids for Flag-β-catenin 4A and TCF4E-V5 were transfected into 293T cells. Cells were then treated with the indicated amounts of chloroxylenol for 24 h, followed by immunoprecipitation using anti-Flag agarose. The interaction between β-catenin 4A and TCF4E was assessed using immunoblotting. (G) HCT116 cells were incubated with DMSO or chloroxylenol for 24 h and then immunoprecipitated using control IgG or anti-β-catenin antibodies. The interaction between β-catenin and TCF4E was determined using immunoblotting. Data are presented as mean ± SD. n=3. *P<0.05 vs. control (0 μM) group. ChIP, chromatin immunoprecipitation.

In vivo inhibition of tumor growth by chloroxylenol in an MC38 cell xenograft model. To further evaluate the *in vivo* anti-tumor effects of chloroxylenol, an MC38 mouse colon cancer xenograft model was used to assess its anti-cancer activity. MC38 cells were subcutaneously injected into C57BL/6 mice and when the tumor volume reached ~50 mm^3, mice were administered either a control solvent or chloroxylenol at 5 mg/kg via intraperitoneal injection on days 0, 2, 4, 6, 8 and 10. Mice were euthanized on day 14 after six treatments, and the tumor volume and weight were measured. Total RNA and protein were extracted from the xenografts and tumor histology was studied. Chloroxylenol exhibited marked inhibitory effects on tumor growth (Fig. 7A). During chloroxylenol treatment process, there were no significant changes in mouse body weight compared with the control group (Fig. 7B). Tumor volume (Fig. 7C) and weight (Fig. 7D) were significantly decreased after chloroxylenol treatment. Histological H&E staining indicated that chloroxylenol treatment markedly reduced tumor cell density (Fig. 7E) compared with the vehicle control. Furthermore, immunohistochemical staining results demonstrated that chloroxylenol markedly suppressed the expression of cancer stemness marker LGR5 in the tumor tissue of the xenografts (Fig. 7F). RT-qPCR analysis further demonstrated that the inhibitory effect of chloroxylenol on Wnt signaling, demonstrated a significant decrease in the mRNA expression levels of Wnt target genes (Fig. 7G).

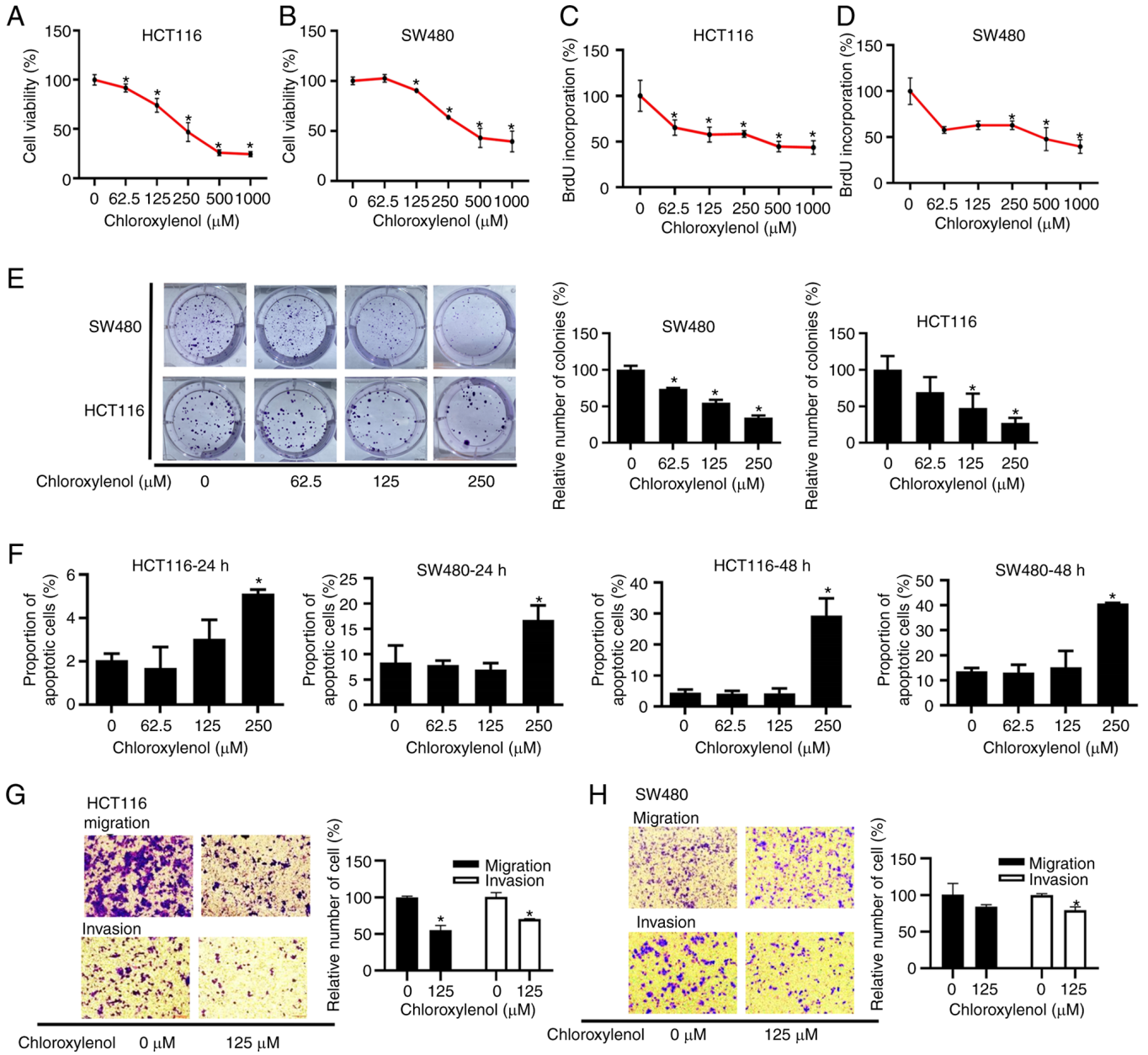

Figure 5. Chloroxylenol promotes apoptosis and suppresses viability, proliferation, migration and invasion in CRC cells. HCT116 and SW480 cells were treated with DMSO or chloroxylenol at the indicated concentrations for 48 h before evaluation of cell viability using an (A and B) MTT assay and (C and D) cell proliferation using a BrdU assay. (E) HCT116 and SW480 cells were treated with the indicated amounts of chloroxylenol for 7 days. Cells were then stained with crystal violet and image. The right panel presented a graphical representation of the quantitative data. (F) HCT116 and SW480 cells were incubated with the indicated concentrations of chloroxylenol for 24 (left) or 48 h (right). Apoptosis was assessed using flow cytometry. The graph shows the percentage of apoptotic cells. (G) HCT116 or (H) SW480 cells were transferred to Transwell chambers with the indicated concentrations of chloroxylenol. The migrated cells were stained and imaged. The invaded cells were stained and imaged. Data are presented as mean ± SD. n=3. *P<0.05 vs. control (0 μM) group.

Moreover, chloroxylenol treatment significantly reduced the protein expression levels of LGR5 and SOX2 (Fig. 7H).

Reduction of organoid formation by chloroxylenol in human CRC tissue samples. To further appraise the effect of chloroxylenol on human colorectal CSCs and the therapeutic benefits for patients with CRC, organoids derived from the CRC patient were developed and used to analyze the effect of chloroxylenol on their growth. The organoids were treated with 125 and 250 μM chloroxylenol. Chloroxylenol treatment inhibited the growth of organoids (Fig. 8A) and markedly reduced the mRNA and protein expression levels of CSC related proteins LGR5 and SOX2 (Fig. 8B and C). These results indicated that chloroxylenol could significantly inhibit the growth of CRC organoids.

Discussion

As a widely used antibacterial and antifungal agent, chloroxylenol has been reported to have antiviral activity in recent years (44). Compared with other antimicrobial ingredients in consumer products, including triclosan, triclocarban, benzalkonium chloride and benzethonium chloride, chloroxylenol has been previously reported to exhibit low acute toxicity, low systemic toxicity, and a lack of genotoxicity and carcinogenicity (45).

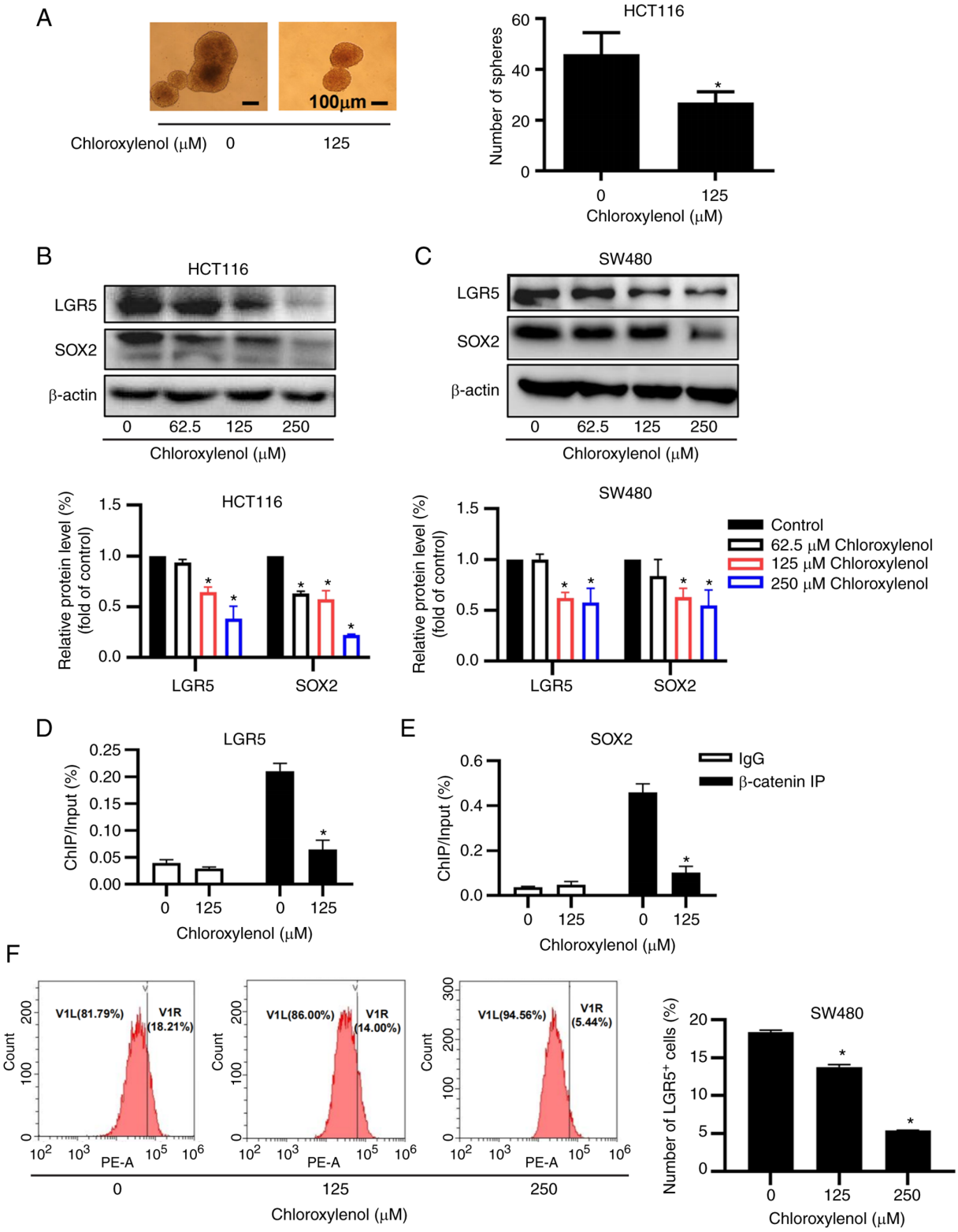

Figure 6. Chloroxylenol suppresses the stemness of CRC cells. (A) Sphere formation of HCT116 cells cultured in Ultra-Low Attachment dishes with or without chloroxylenol treatment. Spheres >50 μm in diameter were counted using a microscope. Relative number of spheres formed by HCT116 cells treated with control or chloroxylenol at the indicated concentrations. (B and C) The protein expression levels of LGR5 and SOX2 were analyzed using western blotting. (D and E) HCT116 cells were treated with chloroxylenol or DMSO for 24 h, followed by cross-linking fixation, immunoprecipitation, affinity purification and quantitative PCR assays for the promoters of LGR5 and SOX2. (F) Flow cytometry results showed the relative number of LGR5-positive cells after chloroxylenol treatment. Data are presented as mean ± SD. n=3. *P<0.05 vs. control (0 μM) group. ChIP, chromatin immunoprecipitation.

Yang *et al* (46) reported that triclosan could increase the severity of colitis symptoms and exacerbated colitis-associated colon cancer cell growth via gut microbiota- and TLR4-dependent mechanisms. Triclocarban has been reported to increase dextran sodium sulfate (DSS) and IL-10 knockout-induced colitis, and to have exaggerated azoxymethane (AOM)/DSS-induced colon

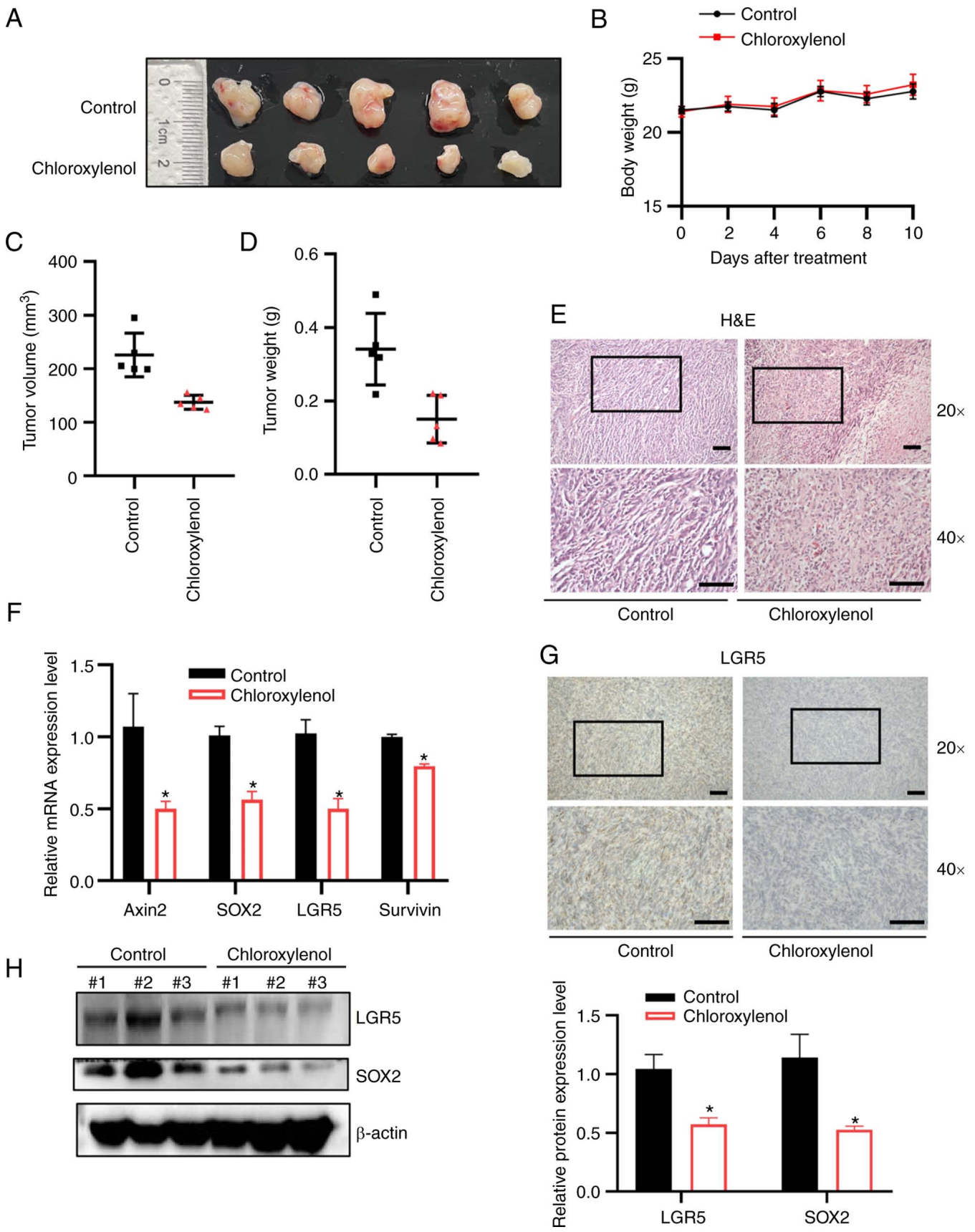

Figure 7. Chloroxylenol inhibits tumor growth in an MC38 mouse colon cancer xenograft model. MC38 xenografts were treated with control solvent or chloroxylenol at 5 mg/kg on days 0, 2, 4, 6, 8 and 10 by intraperitoneally injection. After 6 rounds of treatment, mice were sacrificed on the fourteenth day, and tumors were excised and weighed. (A) Images of tumors from control group and treatment group. (B) Weight of mice after being treated with control solvent or chloroxylenol. (C) Mean tumor volumes. (D) Mean tumor weight. (E) H&E staining of tumor section; scale bar, 200 μm. (G) Immunohistochemical staining of LGR5; scale bar, 200 μm. (F) The mRNA expression levels of the Wnt target genes Axin2, LGR5, SOX2 and Survivin were quantitated using reverse transcription-quantitative PCR. Data are presented as mean ± SD. (H) The protein expression levels of LGR5 and SOX2 in tumor samples were assessed using western blotting. n=5. *P<0.05 vs. control (0 μM) group.

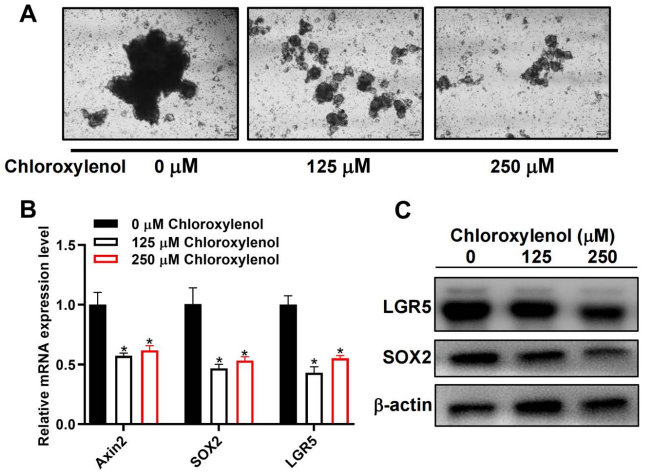

Figure 8. Chloroxylenol inhibits the growth of patient-derived CRC organoids. (A) The colon cancer tissues from CRC patient were purified and cultured in the indicated medium supplemented with chloroxylenol or DMSO. After 7 days, the organoids were imaged under the microscope. (B) Total RNA from the organoids was extracted and reverse transcribed into complementary DNA and the expression of LGR5, SOX2 and Axin2 was assessed using quantitative PCR. (C) The protein expression of LGR5 and SOX2 proteins in organoids was analyzed using western blotting. n=2. Data are presented as mean ± SD. *P<0.05 vs. control (0 μM) group.

tumorigenesis in mice (47). Moreover, exposure to benzalkonium chloride and benzethonium chloride also exaggerated DSS-induced colonic inflammation and AOM/DSS-induced colitis-associated colon tumorigenesis in mice (48). However, compared with benzalkonium chloride and benzethonium chloride, chloroxylenol was reported to have had little effect on DSS-induced colonic inflammation and AOM/DSS-induced colitis-associated colon tumorigenesis in mice (49). It remains unclear why chloroxylenol exerts a different effect on colonic inflammation and colitis-associated colon tumorigenesis compared with other antimicrobial agents.

Inflammatory bowel disease (IBD) is a chronic gastrointestinal inflammatory disorder with an increasing incidence and includes two major forms, Crohn's disease and ulcerative colitis (49). In patients with IBD, the most serious complication is the development of colitis-associated colon cancer (50,51). It has been previously reported that the constitutive activation of canonical Wnt/β-catenin signaling is critical in the initiation and progression of CRC (38). The Wnt/β-catenin signaling pathway is also essential for gut development and homeostasis (52). Significant differences in cell-surface components of the Wnt pathway have been reported in the colonic mucosa of patients with IBD compared with non-IBD patients (53). Moreover, conditional knockout mice that specifically lack the Wnt co-receptor LRP5/6 or β-catenin in $CD11c^+$ antigen-presenting cells developed more severe acute colitis (54). Concerning the importance of Wnt/β-catenin signaling in chronic intestinal inflammation and CRC, the Wnt antagonistic actions of chloroxylenol may at least partially counteract its effect on colonic inflammation and colitis-associated colon tumorigenesis. The present study provided novel insight into the effect of chloroxylenol on colonic inflammation and colitis-associated colon tumorigenesis.

CSCs, also known as tumor-initiating cells, are a subgroup of cancer cells with the ability to self-renew and differentiate into heterogeneous cancer cell lineages and are considered to be responsible for drug resistance and cancer recurrence in multiple forms of cancer including CRC (55,56). Constitutive activation of Wnt signaling has been reported to serve an important role in the growth and maintenance of colorectal CSCs. Colorectal CSCs have also been reported to exert a Wnt/β-catenin signaling high activity (57). In the present study, the antagonistic effect of chloroxylenol on the Wnt/β-catenin signaling pathway was demonstrated. Chloroxylenol inhibited β-catenin nuclear translocation and β-catenin-mediated transcriptional activity and downregulated the expression of Wnt target genes. The inhibitory effect of chloroxylenol on Wnt signaling was demonstrated at concentration comparable to that which demonstrated an inhibitory effect on CRC cells, which indicated that the Wnt inhibitory effect of chloroxylenol was associated with its anti-tumor activity in CRC. Furthermore, the results of the present study demonstrated that chloroxylenol could inhibit colorectal cancer xenograft growth, the sphere-forming ability and organoid formation in CRC, and result in a significant decrease in the expression of the stemness marker genes LGR5 and SOX2. These results indicated that chloroxylenol could selectively inhibit colorectal CSCs through targeting of the Wnt/β-catenin signaling pathway. Further studies are needed to develop chloroxylenol derivatives with lower toxicity and more potent inhibitory effects on Wnt signaling for CRC treatment.

There were certain limitations of the present study due to the utilization of a relatively high concentration range of chloroxylenol to elicit its anticancer effects. This effective dosage, spanning 62.5-250 μM, may engender challenges concerning its translational implementation and further advancement in therapeutic development. Consequently, exploration of the synergistic effects of chloroxylenol in combination with other anticancer agents should be further evaluated to fully exploit the potential of this small molecule targeting the Wnt/β-catenin signaling pathway.

Chloroxylenol is an antimicrobial chemical agent with a long history of safe use in topical antiseptic drug products for over-the-counter human use. The toxicological data for chloroxylenol indicate minimal systemic toxicity, and a lack of genotoxicity and carcinogenicity (45). In the present study, it was demonstrated that chloroxylenol could downregulate the Wnt/β-catenin signaling pathway and inhibit the stemness of CRC cells. Concerning the crucial role of Wnt/β-catenin signaling in development and somatic stem cell biology (58), further research should investigate whether long-term exposure to environmental doses of chloroxylenol has any adverse effects on embryonic development and tissue stem cell behavior in organ systems, including the gut, the hematopoietic system and the nervous system.

Acknowledgements

Not applicable.

Funding

This work was supported by The National Natural Science Foundation of China (grant nos. 31970739 and 82273485), The Natural Science Foundation of Guangdong Province (grant nos. 2020A1515010340 and 2022A1515010598),

The Shenzhen Key Basic Research Program (grant no. JCYJ20200109105001821) and The Shenzhen Natural Science Fund (the Stable Support Plan Program) (grant no. 20200826134656001).

Availability of data and materials

The datasets used and/or analyzed during the current study are available from the corresponding author on reasonable request.

Authors' contributions

QS, GY and DL developed the concept and designed the present study. QS, BL, QL, ZS, QF, LW, CL and YD performed the experiments and data acquisition. QS, BL, VWX, SL, XC and DL performed data analysis. QS and DL edited and revised the manuscript. DL supervised this study. All authors read and approved this manuscript.

Ethics approval and consent to participate

The ethics committee of Shenzhen University approved the research (approval nos. AEWC-2021006 and PN-2022-001).

Patient consent for publication

All patients involved in this study gave consent for the publication of the data.

Competing interests

The authors declare that they have no competing interests.

References

1. Rundle CW, Hu S, Presley CL and Dunnick CA: Triclosen and its alternatives in antibacterial soaps. Dermatitis 30: 352-357, 2019.
2. Sreevidya VS, Lenz KA, Svoboda KR and Ma H: Benzalkonium chloride, benzethonium chloride, and chloroxylenol-three replacement antimicrobials are more toxic than triclosan and triclocarban in two model organisms. Environ Pollut 235: 814-824, 2018.
3. Antunes SC, Nunes B, Rodrigues S, Nunes R, Fernandes J and Correia AT: Effects of chronic exposure to benzalkonium chloride in Oncorhynchus mykiss: Cholinergic neurotoxicity, oxidative stress, peroxidative damage and genotoxicity. Environ Toxicol Pharmacol 45: 115-122, 2016.
4. Food and Drug Adminnistration, HHS: Safety and effectiveness of consumer antiseptics; topical antimicrobial drug products for over-the-counter human use. Final rule. Fed Regist 81: 61106-61130, 2016.
5. Wang J, Shan S, Li D, Zhang Z and Ma Q: Long-term influence of chloroxylenol on anaerobic microbial community: Performance, microbial interaction, and antibiotic resistance gene behaviors. Sci Total Environ 897: 165330, 2023 (Epub ahead of print).
6. Siegel RL, Wagle NS, Cercek A, Smith RA and Jemal A: Colorectal cancer statistics, 2023. CA Cancer J Clin 73: 233-254, 2023.
7. Biller LH and Schrag D: Diagnosis and treatment of metastatic colorectal cancer: A review. JAMA 325: 669-685, 2021.
8. Doubeni CA, Corley DA, Quinn VP, Jensen CD, Zauber AG, Goodman M, Johnson JR, Mehta SJ, Becerra TA, Zhao WK, *et al*: Effectiveness of screening colonoscopy in reducing the risk of death from right and left colon cancer: A large community-based study. Gut 67: 291-298, 2018.
9. Song M, Garrett WS and Chan AT: Nutrients, foods, and colorectal cancer prevention. Gastroenterology 148: 1244-1260. e16, 2015.
10. Lytle NK, Barber AG and Reya T: Stem cell fate in cancer growth, progression and therapy resistance. Nat Rev Cancer 18: 669-680, 2018.
11. Meacham CE and Morrison SJ: Tumour heterogeneity and cancer cell plasticity. Nature 501: 328-337, 2013.
12. Chaffer CL and Weinberg RA: A perspective on cancer cell metastasis. Science 331: 1559-1564, 2011.
13. Yang L, Shi P, Zhao G, Xu J, Peng W, Zhang J, Zhang G, Wang X, Dong Z, Chen F and Cui H: Targeting cancer stem cell pathways for cancer therapy. Signal Transduct Target Ther 5: 8, 2020.
14. Clevers H: The cancer stem cell: Premises, promises and challenges. Nat Med 17: 313-319, 2011.
15. Medema JP: Targeting the colorectal cancer stem cell. N Engl J Med 377: 888-890, 2017.
16. Shimokawa M, Ohta Y, Nishikori S, Matano M, Takano A, Fujii M, Date S, Sugimoto S, Kanai T and Sato T: Visualization and targeting of LGR5^{+} human colon cancer stem cells. Nature 545: 187-192, 2017.
17. Frank MH, Wilson BJ, Gold JS and Frank NY: Clinical implications of colorectal cancer stem cells in the age of single-cell omics and targeted therapies. Gastroenterology 160: 1947-1960, 2021.
18. Batlle E and Clevers H: Cancer stem cells revisited. Nat Med 23: 1124-1134, 2017.
19. Nusse R and Clevers H: Wnt/β-catenin signaling, disease, and emerging therapeutic modalities. Cell 169: 985-999, 2017.
20. MacDonald BT, Tamai K and He X: Wnt/beta-catenin signaling: Components, mechanisms, and diseases. Dev Cell 17: 9-26, 2009.
21. Clevers H and Nusse R: Wnt/β-catenin signaling and disease. Cell 149: 1192-1205, 2012.
22. Cancer Genome Atlas Network: Comprehensive molecular characterization of human colon and rectal cancer. Nature 487: 330-337, 2012.
23. Wood LD, Parsons DW, Jones S, Lin J, Sjöblom T, Leary RJ, Shen D, Boca SM, Barber T, Ptak J, *et al*: The genomic landscapes of human breast and colorectal cancers. Science 318: 1108-1113, 2007.
24. Zhang L and Shay JW: Multiple roles of APC and its therapeutic implications in colorectal cancer. J Natl Cancer Inst 109: djw332, 2017.
25. Krishnamurthy N and Kurzrock R: Targeting the Wnt/beta-catenin pathway in cancer: Update on effectors and inhibitors. Cancer Treat Rev 62: 50-60, 2018.
26. Bilic J, Huang YL, Davidson G, Zimmermann T, Cruciat CM, Bienz M and Niehrs C: Wnt induces LRP6 signalosomes and promotes dishevelled-dependent LRP6 phosphorylation. Science 316: 1619-1622, 2007.
27. Gao C and Chen YG: Dishevelled: The hub of Wnt signaling. Cell Signal 22: 717-727, 2010.
28. Valenta T, Hausmann G and Basler K: The many faces and functions of β-catenin. EMBO J 31: 2714-2736, 2012.
29. Behrens J, von Kries JP, Kühl M, Bruhn L, Wedlich D, Grosschedl R and Birchmeier W: Functional interaction of beta-catenin with the transcription factor LEF-1. Nature 382: 638-642, 1996.
30. Doumpas N, Lampart F, Robinson MD, Lentini A, Nestor CE, Cantù C and Basler K: TCF/LEF dependent and independent transcriptional regulation of Wnt/β-catenin target genes. EMBO J 38: e98873, 2019.
31. Poger D and Mark AE: Effect of triclosan and chloroxylenol on bacterial membranes. J Phys Chem B 123: 5291-5301, 2019.
32. Cutts TA, Ijaz MK, Nims RW, Rubino JR and Theriault SS: Effectiveness of dettol antiseptic liquid for inactivation of Ebola virus in suspension. Sci Rep 9: 6590, 2019.
33. Nowak M, Zawadzka K, Szemraj J, Góralczyk-Bińkowska A and Lisowska K: Biodegradation of chloroxylenol by cunninghamella elegans IM 1785/21GP and trametes versicolor IM 373: Insight into ecotoxicity and metabolic pathways. Int J Mol Sci 22: 4360, 2021.
34. Wang Z, Zhou L, Xiong Y, Yu S, Li H, Fan J, Li F, Su Z, Song J, Sun Q, *et al*: Salinomycin exerts anti-colorectal cancer activity by targeting the β-catenin/T-cell factor complex. Br J Pharmacol 176: 3390-3406, 2019.
35. Livak KJ and Schmittgen TD: Analysis of relative gene expression data using real-time quantitative PCR and the 2(-Delta Delta C(T)) method. Methods 25: 402-408, 2001.
36. Wang L, Deng K, Gong L, Zhou L, Sayed S, Li H, Sun Q, Su Z, Wang Z, Liu S, *et al*: Chlorquinaldol targets the β-catenin and T-cell factor 4 complex and exerts anti-colorectal cancer activity. Pharmacol Res 159: 104955, 2020.

37. Sun Q, Wang Y, Fu Q, Ouyang A, Liu S, Wang Z, Su Z, Song J, Zhang Q, Zhang P and Lu D: Sulfur-coordinated organoiridium(III) complexes exert breast anticancer activity via inhibition of Wnt/β-catenin signaling. Angew Chem Int Ed Engl 60: 4841-4848, 2021.
38. Zhao H, Ming T, Tang S, Ren S, Yang H, Liu M, Tao Q and Xu H: Wnt signaling in colorectal cancer: Pathogenic role and therapeutic target. Mol Cancer 21: 144, 2022.
39. Hagen T, Di Daniel E, Culbert AA and Reith AD: Expression and characterization of GSK-3 mutants and their effect on beta-catenin phosphorylation in intact cells. J Biol Chem 277: 23330-23335, 2002.
40. Xu C, Xu Z, Zhang Y, Evert M, Calvisi DF and Chen X: β-Catenin signaling in hepatocellular carcinoma. J Clin Invest 132: e154515, 2022.
41. Su Z, Song J, Wang Z, Zhou L, Xia Y, Yu S, Sun Q, Liu SS, Zhao L, Li S, *et al*: Tumor promoter TPA activates Wnt/β-catenin signaling in a casein kinase 1-dependent manner. Proc Natl Acad Sci USA 115: E7522-E7531, 2018.
42. Bazzi H, Fantauzzo KA, Richardson GD, Jahoda CA and Christiano AM: The Wnt inhibitor, Dickkopf 4, is induced by canonical Wnt signaling during ectodermal appendage morphogenesis. Dev Biol 305: 498-507, 2007.
43. Lundberg IV, Edin S, Eklöf V, Öberg Å, Palmqvist R and Wikberg ML: SOX2 expression is associated with a cancer stem cell state and down-regulation of CDX2 in colorectal cancer. BMC Cancer 16: 471, 2016.
44. Dellanno C, Vega Q and Boesenberg D: The antiviral action of common household disinfectants and antiseptics against murine hepatitis virus, a potential surrogate for SARS coronavirus. Am J Infect Control 37: 649-652, 2009.
45. Yost LJ, Rodricks JD, Turnbull D, DeLeo PC, Nash JF, Quiñones-Rivera A and Carlson PA: Human health risk assessment of chloroxylenol in liquid hand soap and dishwashing soap used by consumers and health-care professionals. Regul Toxicol Pharmacol 80: 116-124, 2016.
46. Yang H, Wang W, Romano KA, Gu M, Sanidad KZ, Kim D, Yang J, Schmidt B, Panigrahy D, Pei R, *et al*: A common antimicrobial additive increases colonic inflammation and colitis-associated colon tumorigenesis in mice. Sci Transl Med 10: eaan4116, 2018.
47. Yang H, Sanidad KZ, Wang W, Xie M, Gu M, Cao X, Xiao H and Zhang G: Triclocarban exposure exaggerates colitis and colon tumorigenesis: Roles of gut microbiota involved. Gut Microbes 12: 1690364, 2020.
48. Sanidad KZ, Yang H, Wang W, Ozay EI, Yang J, Gu M, Karner E, Zhang J, Kim D, Minter LM, *et al*: Effects of consumer antimicrobials benzalkonium chloride, benzethonium chloride, and chloroxylenol on colonic inflammation and colitis-associated colon tumorigenesis in mice. Toxicol Sci 163: 490-499, 2018.
49. Kaplan GG: The global burden of IBD: From 2015 to 2025. Nat Rev Gastroenterol Hepatol 12: 720-727, 2015.
50. Rogler G: Chronic ulcerative colitis and colorectal cancer. Cancer Lett 345: 235-241, 2014.
51. Rubin DC, Shaker A and Levin MS: Chronic intestinal inflammation: Inflammatory bowel disease and colitis-associated colon cancer. Front Immunol 3: 107, 2012.
52. Tian A, Benchabane H and Ahmed Y: Wingless/Wnt signaling in intestinal development, homeostasis, regeneration and tumorigenesis: A drosophila perspective. J Dev Biol 6: 8, 2018.
53. You J, Nguyen AV, Albers CG, Lin F and Holcombe RF: Wnt pathway-related gene expression in inflammatory bowel disease. Dig Dis Sci 53: 1013-1019, 2008.
54. Swafford D, Shanmugam A, Ranganathan P, Hussein MS, Koni PA, Prasad PD, Thangaraju M and Manicassamy S: Canonical Wnt signaling in $CD11c^{+}$ APCs regulates microbiota-induced inflammation and immune cell homeostasis in the colon. J Immunol 200: 3259-3268, 2018.
55. Shlush LI, Mitchell A, Heisler L, Abelson S, Ng SWK, Trotman-Grant A, Medeiros JJF, Rao-Bhatia A, Jaciw-Zurakowsky I, Marke R, *et al*: Tracing the origins of relapse in acute myeloid leukaemia to stem cells. Nature 547: 104-108, 2017.
56. Phi LTH, Sari IN, Yang YG, Lee SH, Jun N, Kim KS, Lee YK and Kwon HY: Cancer stem cells (CSCs) in drug resistance and their therapeutic implications in cancer treatment. Stem Cells Int 2018: 5416923, 2018.
57. Katoh M and Katoh M: WNT signaling and cancer stemness. Essays Biochem 66: 319-331, 2022.
58. Ring A, Kim YM and Kahn M: Wnt/catenin signaling in adult stem cell physiology and disease. Stem Cell Rev Rep 10: 512-525, 2014.